

Precision of Inflaton Potential Reconstruction from CMB Using the General Slow-Roll Approximation

Kenji Kadota¹, Scott Dodelson^{1,2,3}, Wayne Hu^{2,4} and Ewan D. Stewart^{5,6*}

¹ Particle Astrophysics Center, Fermi National Accelerator Laboratory, Batavia, IL 60510, USA

²Department of Astronomy & Astrophysics, The University of Chicago, Chicago, IL 60637, USA

³Department of Physics and Astronomy, Northwestern University, Evanston, IL 60208

⁴ Kavli Institute for Cosmological Physics, The University of Chicago, Chicago, IL 60637, USA

⁵Department of Physics, KAIST, Daejeon 305-701, Republic of Korea *and*

⁶Canadian Institute for Theoretical Astrophysics,
University of Toronto, Toronto, ON M5S 3H8, Canada

Through a principal component analysis, we study how accurately CMB observables can constrain inflaton potentials in a model independent manner. We apply the general slow-roll approximation in our analysis where we allow, in contrast to the standard slow-roll approximation, the possibility of variations in $V''(\phi)$ and take into account the fact that horizon crossing is not an instantaneous event. Our analysis provides a set of modes to be used in fitting observables. We find that of order five of these modes will be constrained by future observations, so a fully general data analysis package could use the amplitudes of just a handful of modes as free parameters and retain all relevant information in the data.

I. INTRODUCTION

The origin of cosmic density perturbations is one of the most notable predictions of the inflationary scenario. The observational data on their power spectrum from the cosmic microwave background (CMB) and large scale structure provide us with one of few windows through which we can probe the physics governing the early Universe [1, 2, 3, 4]. In particular it is interesting to ask if the CMB can directly constrain the potential energy of the field driving inflation, the *inflaton*, and if so, which features of the potential will be most accurately measured. Extracting the physics of inflation from CMB data alone is not trivial because different inflation models can produce identical CMB spectra and moreover CMB observables can cover only a tiny portion of an inflaton potential. However, we can still try to constrain the curvature, for example, of the inflaton potential during the time when cosmologically interesting scales were exiting the horizon, and the sign of the curvature alone can already distinguish between several classes of inflation models. Because we are still not certain of the functional form of the inflaton potential, it would be useful

to work in a model-independent manner to avoid biasing our estimates of the properties of inflaton potentials. Further, we are motivated to ask what other features of the potential are constrained by the CMB, again in a model-independent way?

There exist many works which reconstruct the primordial power spectrum $\mathcal{P}(k)$ from the observable CMB data C_l (see, for example, [5, 6, 7, 8, 9, 10, 11] for model-independent approaches). If we can also measure the tensor perturbations and assume the standard slow-roll approximation, reconstructing the inflaton potential is feasible [12]. Even without the standard slow-roll approximation, the conversion from $\mathcal{P}(k)$ to inflaton potential parameters is possible analytically for a given $\mathcal{P}(k)$ [13, 14]. So we could combine these analyses to examine the properties of inflation from C_l by two steps: $C_l \rightarrow \mathcal{P}(k) \rightarrow$ inflaton potential parameters. However, degeneracies between the parameters arise from these two steps, and it would be more efficient to constrain an inflaton potential directly from C_l . If we perform a numerical analysis such as the Markov Chain Monte Carlo method, reconstructing the inflaton potential directly from C_l can be done without heavily relying on the standard slow-roll approximation [15, 16]. However, even in the case of numerical analysis, how many inflaton potential parameters do we need in addition to cosmological parameters such as the reionization optical depth and baryon density? Certainly including more pa-

*On sabbatical leave from Department of Physics, KAIST, Republic of Korea.

rameters would lead to a better fit to observations, but adding as many free parameters as we want would not be a practical approach. Our principal component analysis will be useful in choosing an optimal set of parameters to characterize the inflaton potential.

In Sec. II we describe the general slow-roll approximation with an emphasis on the difference from the standard slow-roll approximation, and discuss a model-independent parametrization of the inflaton potential. Sec. III outlines a principal component analysis and determines the precision that idealized future CMB experiments can attain in constraining inflaton potential parameters. Sec. IV gives some illustrations of the formalism, followed by the conclusion in Sec. V.

II. INFLATON POTENTIAL PARAMETRIZATION

We, in this section, discuss a model independent parametrization of the inflaton potential (strictly speaking, a function of the inflaton potential) which appears in the expression of cosmological power spectra in the general slow-roll approximation.

A. General Slow-Roll Approximation

One of the possible pitfalls of the standard slow-roll approximation is that it presumes the scale invariance of $V''(\phi)$. For single field inflation with slow-roll, the observations are indeed consistent with a small amplitude¹ of V'' . Neither observations nor theories, however, require exact scale invariance. The general slow-roll approximation can lift this extra (and unnecessary) condition of the scale invariance of V'' [17]. Another pitfall of the standard slow-roll calculations is the matching condition at “horizon crossing” $k = \mathcal{O}(1)aH$ where one conventionally just evaluates the perturbations exactly at $k = aH$. The $\mathcal{O}(1)$ ambiguity in the “horizon crossing” [18] and also the possible prolonged effects around horizon crossing are accounted for in the general slow-roll approximation. Under the general slow-roll approximation, the power spectrum for a single field inflation model² is given

as

$$\begin{aligned} \ln \mathcal{P}(\ln k) &= \int_0^\infty \frac{d\xi}{\xi} [-k\xi W'(k\xi)] \left[\ln \frac{1}{f^2} + \frac{2}{3} \frac{f'}{f} \right] \\ &\equiv \int_0^\infty \frac{d\xi}{\xi} [-k\xi W'(k\xi)] G(\ln \xi), \end{aligned} \quad (1)$$

where ξ , minus the conformal time, is an integral over the scale factor a up to the end of inflation:

$$\xi \equiv - \int_t^{t_{\text{end}}} \frac{dt'}{a(t')}. \quad (2)$$

$W(x)$ is given as

$$W(x) = \frac{3 \sin(2x)}{2x^3} - \frac{3 \cos(2x)}{x^2} - \frac{3 \sin(2x)}{2x}, \quad (3)$$

so that the window function $-xW'(x)$ in Eq. (1) is

$$-xW'(x) = -\frac{3(5x^2 - 3)}{2x^3} \sin(2x) + \frac{3(x^2 - 3)}{x^2} \cos(2x), \quad (4)$$

and the normalization is such that

$$\int_0^\infty \frac{dx}{x} [-xW'(x)] = 1. \quad (5)$$

The dependence on the dynamics of the inflaton field is encoded in

$$f(\ln \xi) \equiv \frac{2\pi a \xi \dot{\phi}}{H}, \quad (6)$$

where H is the Hubble constant and $\dot{\phi} = d\phi/dt$ is the time derivative of the inflaton field. Here and below primes denote derivatives with respect to the argument, e.g. $f' = df/d\ln \xi$. $\xi = (aH)^{-1}[1 + \mathcal{O}(\dot{H}/H^2)]$, so, to the leading order, $f = 2\pi\dot{\phi}/H^2$ which is just an inverse of the familiar comoving curvature perturbation. The amplitude of f'/f is small in the general slow-roll approximation as well as in the standard slow-roll approximation. f'/f can, however, vary rapidly in the general slow-roll approximation in contrast to the case of the standard slow-roll approximation.

As we can see from the integral over $d\ln \xi$ in Eq. (1), the power spectrum receives contributions from a range of ξ for a given mode k , not only the one moment of horizon crossing as in the standard slow-roll formula. This is because a given Fourier mode is affected by the inflationary dynamics over the whole period it is leaving the horizon, not just at one instant; these details are specified by the properties of the window function $-k\xi W'(k\xi)$ which is shown in Fig. 1. The mode oscillates rapidly inside the horizon (when $k\xi \gg 1$), and one would need

¹ We use units in which $8\pi G = 1$.

² In this paper, we consider only single field inflation models.

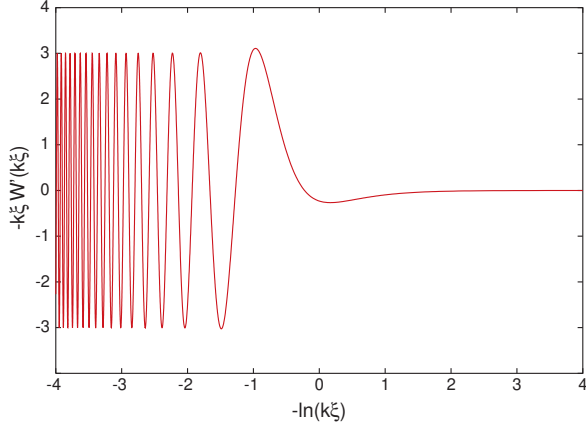


FIG. 1: The window function for the general slow-roll formula $-k\xi W'(k\xi)$ as the function of $-\ln(k\xi)$. Large $k\xi$ corresponds to earlier times, when the mode of interest is within the horizon, so time flows from left to right.

a sudden event to affect it. The window function starts to vanish for $k\xi < 1$ once the mode leaves the horizon because it freezes out and becomes hard to affect. For a slowly varying f' as in the case of the standard slow-roll, the window function is not resolved and just appears as a delta function. Then, Eq. (1) reduces to $\mathcal{P} = 1/f^2 = (H^2/2\pi\dot{\phi})^2$, the standard result [19, 20].

We now consider a model-independent parametrization of the inflaton potential in view of the general slow-roll approximation to study how precisely CMB observations can ultimately constrain the inflaton potential.

B. Discrete Parametrization

Scalar perturbations alone cannot constrain V itself (we need tensor perturbations to do it) but rather certain functions of V . In this paper, we consider the physical limitations of CMB observables without tensor perturbations for constraining

$$3\left(\frac{V'}{V}\right)^2 - 2\frac{V''}{V} . \quad (7)$$

With the standard slow-roll approximation, the spectral index is directly related to this quantity $n - 1 = -3(V'/V)^2 + 2V''/V$. This simple relation for the spectral index is not valid anymore for the general slow-roll cases, but this expression is still a physically fundamental quantity representing an inflaton potential even for the general slow-roll cases. Indeed the integrand in the

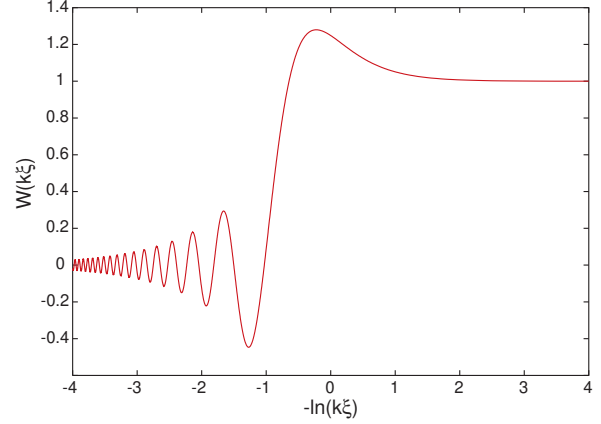


FIG. 2: The window function $W(k\xi)$ as the function of $-\ln(k\xi)$

general slow-roll formula Eq. (1) reduces to

$$\begin{aligned} \frac{d}{d\ln\xi} G(\ln\xi) &\equiv \frac{d}{d\ln\xi} \left(\ln \frac{1}{f^2} + \frac{2}{3} \frac{f'}{f} \right) \\ &= \frac{2}{3} \left(\frac{f''}{f} - 3 \frac{f'}{f} - \frac{f'^2}{f^2} \right) \\ &= \frac{2}{3} \left(\frac{f''}{f} - 3 \frac{f'}{f} \right) \quad \text{to the leading order} \\ &= 3 \left(\frac{V'}{V} \right)^2 - 2 \frac{V''}{V}, \end{aligned} \quad (8)$$

which is true even if V'' changes with ξ [17].

CMB observables cover less than 10 e-folds in practice corresponding to a small portion of a whole inflaton potential. We therefore, in our analysis, parametrize the inflaton potential across a range greater than 10 e-folds $\xi_{\min} \leq \xi \leq \xi_{\max}$ to ensure it covers the horizon crossing for observable modes. The right hand side of Eq. (1) can then be reduced to

$$\ln \mathcal{P} = \int_{\xi_{\min}}^{\xi_{\max}} \frac{d\xi}{\xi} [-k\xi W'(k\xi)] G(\ln\xi), \quad (9)$$

with negligible contributions from ξ outside the limits of integration which can be justified from $W'(k\xi) \rightarrow 0$ for the large enough ξ_{\max} and the small enough ξ_{\min} . Integrating by parts,

$$\begin{aligned} \ln \mathcal{P} &= -[W(k\xi)G(\ln\xi)]_{\xi_{\min}}^{\xi_{\max}} \\ &+ \int_{\xi_{\min}}^{\xi_{\max}} \frac{d\xi}{\xi} W(k\xi) \frac{dG(\ln\xi)}{d\ln\xi}. \end{aligned} \quad (10)$$

$W(k\xi)$ as the function of $-\ln(k\xi)$ is shown in Fig. 2. $W \rightarrow 0$ for the large enough ξ_{\max} and $W \rightarrow 1$ for the

small enough ξ_{\min} so that

$$\ln \mathcal{P} = G(\ln \xi_{\min}) + \int_{\xi_{\min}}^{\xi_{\max}} \frac{d\xi}{\xi} W(k\xi) \frac{dG(\ln \xi)}{d \ln \xi}. \quad (11)$$

We can also interpret $-dG/d \ln \xi$ as a source function for $n-1$ with the window function $-k\xi W'(k\xi)$ which is clear by taking the derivative of the above expression as follows

$$n-1 \equiv \frac{d \ln \mathcal{P}}{d \ln k} \quad (12)$$

$$= \int_{\xi_{\min}}^{\xi_{\max}} \frac{d\xi}{\xi} [-k\xi W'(k\xi)] \left[-\frac{dG(\ln \xi)}{d \ln \xi} \right]. \quad (13)$$

We choose the fiducial model to be a flat inflaton potential which leads to $dG/d \ln \xi = 0$ and study how precisely we can constrain deviations from $dG/d \ln \xi = 0$. We parametrize these deviations as

$$\frac{dG(\ln \xi)}{d \ln \xi} \equiv \sum_i p_i B_i(\ln \xi), \quad (14)$$

where $\{p_i\}$ form a discrete set of parameters and $B_i(\ln \xi)$ are defined as

$$B_i(\ln \xi) = \begin{cases} 1 & \text{if } \ln \xi_i < \ln \xi \leq \ln \xi_{i+1}, \\ 0 & \text{otherwise.} \end{cases} \quad (15)$$

We choose a discrete representation rather than a continuous one through smooth functions because, in addition to its simplicity, the discontinuities in $dG(\ln \xi)/d \ln \xi$ will not show up in \mathcal{P} due to the window $W(k\xi)$. In practice, we choose a sufficiently fine discretization that the principal components of Sec. III have converged.

With this parameterization, the power spectrum reads

$$\ln \mathcal{P} = G(\ln \xi_{\min}) + \int_{\xi_{\min}}^{\xi_{\max}} \frac{d\xi}{\xi} W(k\xi) \sum_i p_i B_i(\ln \xi), \quad (16)$$

where the fiducial model has the power spectrum amplitude of

$$\mathcal{P}|_{\text{fid}} = \exp[G(\ln \xi_{\min})] = \frac{1}{f_0^2} = (5.07 \times 10^{-5})^2. \quad (17)$$

Here ‘fid’ denotes that it is to be evaluated for the fiducial model (*i.e.* $p_i = 0$).

In Fig. 3 we plot the infinitesimal response in the primordial power spectra to the inflation parameter $\partial \ln \mathcal{P}(k)/\partial p_i$ evaluated for our fiducial model. Note that as might be expected the response takes the form of a localized change in the amount of low vs high k power or ‘tilt’ surrounding horizon crossing $k\xi \sim 1$.

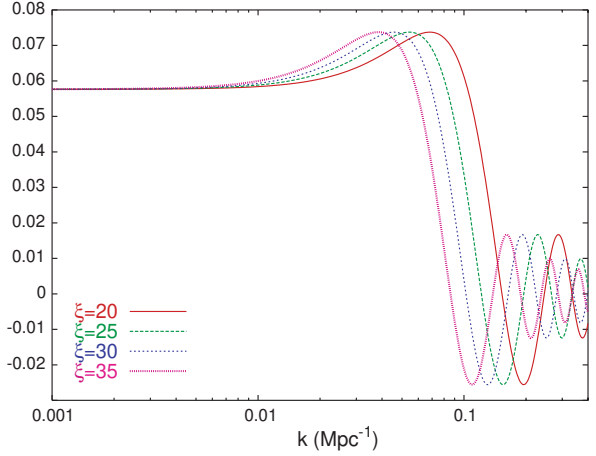


FIG. 3: The response function $\partial \ln \mathcal{P}(k)/\partial p_i$ as the function of $k(\text{Mpc}^{-1})$. The plots are given for four values of p_i whose corresponding ξ values are indicated.

The CMB angular power spectra are given by integrals over \mathcal{P}

$$\frac{l(l+1)C_l^{XX'}}{2\pi} = \int d \ln k T_l^X(k) T_l^{X'}(k) \mathcal{P}(k), \quad (18)$$

where $T_l^X(k)$ are the CMB transfer functions with X representing the CMB temperature or E polarization (*i.e.* X is T or E). For the numerical analysis in Sec. III, we shall oversample the transfer function with 3750 logarithmically spaced k modes from $k = 10^{-4.35} - 10^{-1.35} \text{ Mpc}^{-1}$ and 2500 k modes from $k = 10^{-1.35} - 10^{-0.35} \text{ Mpc}^{-1}$ (see [5] for details). The infinitesimal response in the observable power spectrum to p_i , which will appear in the calculation of the Fisher matrix, is

$$\left. \frac{\partial C_l^{XX'}}{\partial p_i} \right|_{\text{fid}} = \frac{2\pi}{l(l+1)} \int d \ln k T_l^X(k) T_l^{X'}(k) \frac{1}{f_0^2} \times \int_{\xi_{\min}}^{\xi_{\max}} \frac{d\xi}{\xi} W(k\xi) B_i(\ln \xi). \quad (19)$$

We now apply Fisher matrix analysis to calculate the precision to which the $\{p_i\}$ can be constrained to see the physical limitations for future CMB data in reconstructing the inflaton potential.

III. PRINCIPAL COMPONENT ANALYSIS

The Fisher matrix analysis is useful for forecasting the uncertainties in parameter estimation, and we apply it to extract the information on an inflaton potential from

C_l . Assuming a Gaussian distribution for C_l , the Fisher matrix is given by [21]

$$F_{\mu\nu} = \sum_{l=2}^{l_{max}} \sum_{X,Y} \frac{\partial C_l^X}{\partial p_\mu} \mathbf{Cov}^{-1}(C_l^X C_l^Y) \frac{\partial C_l^Y}{\partial p_\nu}, \quad (20)$$

where X, Y represent CMB temperature, E polarization or their cross correlation, and \mathbf{Cov}^{-1} is the inverse of the covariance matrix of the power spectrum C_l . $\{p_\mu\}$ consists of the inflaton potential parameters $\{p_i\}$ and the cosmological parameters which are marginalized over: the dark energy density, equation of state parameter, reionization optical depth and the matter and baryon density with their corresponding fiducial values $\Omega_{DE} = 0.72$, $w = -1$, $\tau = 0.17$, $\Omega_m h^2 = 0.145$ and $\Omega_b h^2 = 0.024$ respectively. We additionally take the overall amplitude of the spectrum f_0 as a parameter. This marginalization can circumvent the possible degeneracies between inflationary and cosmological parameters. For quantifying the physical limitations of inflaton potential reconstruction, we consider ideal, cosmic variance limited observations for both temperature and E polarization measurements out to $l_{max} = 2000$.

The inverse Fisher matrix approximates the covariance matrix $\mathbf{C}(\approx \mathbf{F}^{-1}; \text{Kramer-Rao identity})$ and the marginalized 1- σ error $\sigma(p_\mu)$ for a given parameter p_μ is

$$\sigma(p_\mu) = \sqrt{(\mathbf{C})_{\mu\mu}} \approx \sqrt{(\mathbf{F}^{-1})_{\mu\mu}}. \quad (21)$$

The errors in the individual parameters p_i are in general large and highly correlated to one another in part because under the general slow-roll approximation \mathcal{P} picks up contributions ‘around’ horizon crossing not ‘at’ horizon crossing for each mode. This hinders the interpretation of what aspects of the potential the data will in fact constrain. Moreover the large number of discrete parameters $\{p_i\}$ would make a likelihood search with actual data unfeasible.

We therefore instead apply a principal component analysis. Instead of $\{p_i\}$, we consider a new set of parameters $\{m_i\}$ which are linear combinations of $\{p_i\}$

$$m_a = [\Delta \ln \xi]^{1/2} \sum_i S_{ia} p_i. \quad (22)$$

The normalization factor of $\sqrt{\Delta \ln \xi}$, which depends on the discretization of $\ln \xi$, is chosen so that the variance of m_a is independent of this spacing when it is integrated over $\ln \xi$. As long as the same convention is used for the signal and noise, though, the normalization is arbitrary. The S_{ia} are orthonormal eigenvectors of the covariance

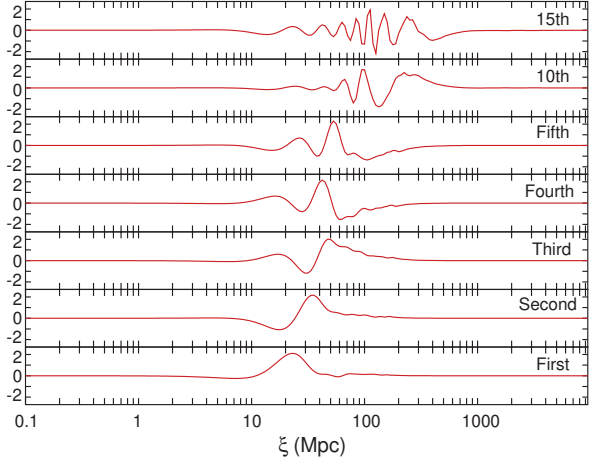


FIG. 4: First five, 10th and 15th best principal components as the function of the minus conformal time ξ .

matrix of the inflation parameters of interest C_{ij} (which is a sub-block of $C_{\mu\nu}$)

$$\sum_j C_{ij} S_{ja} = \frac{1}{\Delta \ln \xi} \sigma_a^2 S_{ia}. \quad (23)$$

Therefore, in our normalization the principle components $S_{ia}/\sqrt{\Delta \ln \xi}$ are normalized to unit variance when integrated over $\ln \xi$

$$\begin{aligned} \int d \ln \xi \left[\frac{S_{ia}}{\sqrt{\Delta \ln \xi}} \right]^2 &= \Delta \ln \xi \sum_i \left[\frac{S_{ia}}{\sqrt{\Delta \ln \xi}} \right]^2 \\ &= 1. \end{aligned} \quad (24)$$

The $\{m_a\}$ are orthogonal (*i.e.* statistically independent) and their covariance matrix becomes a diagonal matrix with the elements

$$\langle m_a m_b \rangle = \sigma_a^2 \delta_{ab}. \quad (25)$$

We consider the parametrization of $dG(\ln \xi)/d \ln \xi$ as given in Eq. (8) for the ξ range of $10^{-1} < \xi/\text{Mpc} < 10^4$, and divide it into 200 equally spaced bins in $\ln \xi$ with 200 parameters $\{p_i\}$ as given by Eq. (14). The principal component decomposition represented by Eq. (22) pinpoints the directions in the parameter space of $\{p_i\}$ with the smallest variances.

These normalized modes $S_{ia}/\sqrt{\Delta \ln \xi}$ are shown in Fig. 4 which plots the five most tightly constrained principal components of the covariance matrix of the inflationary parameters (with the cosmological parameters marginalized over) as well as 10th and 15th ones. Fig. 5 shows the rms error σ_a on the mode amplitudes.

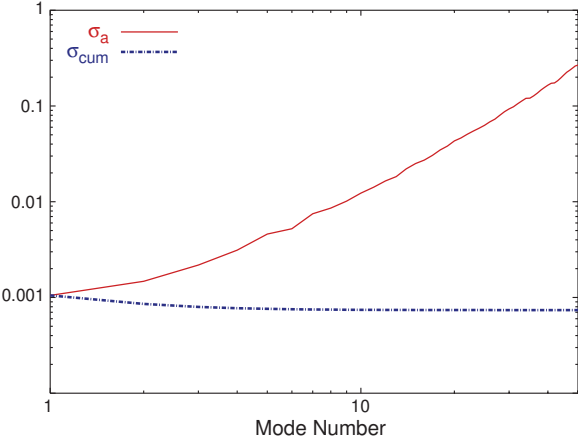


FIG. 5: RMS error on each principal component as the function of mode number. Also shown is the square root of the cumulative variance defined in Eq. (26).

Since the principal components are all normalized to unit variance their joint constraining power can be estimated from the cumulative variance

$$\frac{1}{\sigma_{\text{cum}}^2} = \sum_a \frac{1}{\sigma_a^2}. \quad (26)$$

Fig. 5 shows that only the first handful of modes contribute to the cumulative variance, so we expect these to be the only ones worth including in an analysis. In the next section, we will look at some specific models and see that, practically speaking, this holds true: all the information that can be profitably used to compare theory with observations is contained in the first few modes.

Note that ξ is given in comoving Mpc and its relationship to the number of e-folds from the inflationary era to the present remains undetermined and heavily model dependent. However we can see that the first five eigenmodes are sensitive to the range of $10 \lesssim \xi/\text{Mpc} \lesssim 500$ which covers $\sim \ln 50 \sim 4$ e-folds. This order of magnitude is consistent with our expectation from $\sim \ln l_{\text{max}} = 7.6$ and the high cosmic variance of the low l modes.

Comparing the values of ξ in Fig. 4 and Fig. 3 we can infer that the first eigenmode represents the local tilt around $k \sim 0.1 \text{ Mpc}^{-1}$, which makes sense since the tilt or spectral index would be the best constrained aspect of $\mathcal{P}(k)$. This is what we would expect because $dG(\ln \xi)/d \ln \xi$, which we parametrize here, represents the tilt as we discussed in Sec. II B.

Indeed, if we marginalize over the tilt n as well, the first eigenmode of Fig. 4 disappears, as shown in Fig. 6. We can also infer that the second eigenmode, which has compensating contributions of opposite sign represents

the local running (*i.e.* the difference or change in the local tilt).

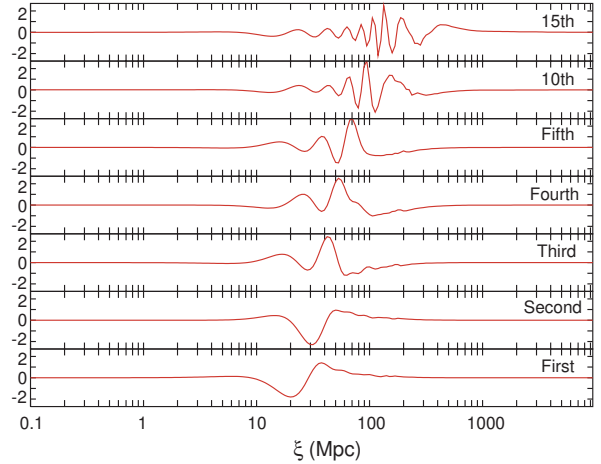


FIG. 6: The best principal components when the tilt n is marginalized over. To be compared with Fig. 4 where n is not included in the marginalized cosmological parameters.

Although these statements remain true for all models, understanding how constraints on the principal components translate into more direct statements about specific models is more difficult. We illustrate their utility in the next section with examples.

IV. EXAMPLES

We now apply the above formalism to two simple examples. These examples serve two purposes: (i) they demonstrate how a generally scale-dependent $n - 1$ is mapped onto the modes defined above and (ii) they illustrate that only the top five or so modes are likely to have signal to noise greater than one. This means that, for the purposes of comparing with CMB observations at least, one can parametrize inflationary models with only five numbers, the amplitudes of the leading modes.

The first example is a trivial one: suppose $n - 1$ is a constant, independent of scale. For concreteness, we choose $n = 0.95$. Then $dG/d \ln \xi = 0.05$; thus all the p_i 's defined in Eq. (14) are equal to 0.05. Although G' in this model is trivial, the eigenvalues m_a – which are the convolution of p_i with the eigenvectors depicted in Figure 4 – are not. Figure 7 shows the first thirty of these.

This example shows that every inflation model can be expressed as a set of m_a . Because each m_a is independent, we can obtain the total signal to noise by

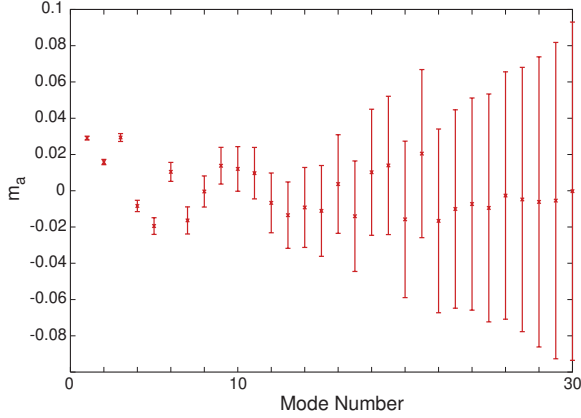


FIG. 7: The first 30 eigenmodes for a potential which produces constant spectral index $n = 0.95$. Error bars are the eigenvalues σ_a ; note that only the first few modes have signal to noise greater than one.

calculating $\sqrt{\sum_i m_i^2 / \sigma_i^2}$. We found, for this example of $n - 1 = -0.05$, $\sum_{i=1}^{2000} m_i^2 / \sigma_i^2 = 1102$ which gives us the estimate of $n - 1 \approx -0.05(1 \pm 1/\sqrt{1102}) = -0.05 \pm 0.0015$. This can be compared with the variance of n obtained directly from the Fisher matrix (where n is taken as the only inflation parameter). In this case, we find $\sigma(n) = 0.0015$, in perfect agreement with the more general approach. We also found that including only the first five modes in the calculation of total signal to noise gives $\sum_{i=1}^5 m_i^2 / \sigma_i^2 = 1088$. Hence, as long as the top five modes are retained, we retain essentially all the information about n . If we knew that n were constant of course, it would be better to use the constant n as the variable to be compared with data.

For more general cases including the case of a variable V'' , the proper way to fit the data would be to allow the best constrained optimal eigenvalues, more specifically five optimal ones, to be free parameters. Our next example demonstrates that this does in fact work.

Consider a perturbation at $\phi = \phi_0$ in an inflaton potential represented by a smooth bump

$$V(\phi) = V_0 e^{\lambda(\phi-\phi_0)} [1 + ce^{-\nu^2(\phi-\phi_0)^2}] \quad (27)$$

where $|\lambda| \ll 1, |c| \ll 1, |\nu| \gg 1$. We now have

$$\begin{aligned} \frac{d\phi}{d\ln(aH)} &= -\frac{V'}{V} \left[1 + \mathcal{O}\left(\frac{V'^2}{V^2}\right) \right] \\ &= -\lambda \quad \text{to the leading order} \end{aligned} \quad (28)$$

so that $\phi \simeq \lambda \ln \xi$ (an integration factor is scaled into ξ such that $\phi_0 = \lambda \ln \xi_0$.) Eqs. (27) and (28) can be

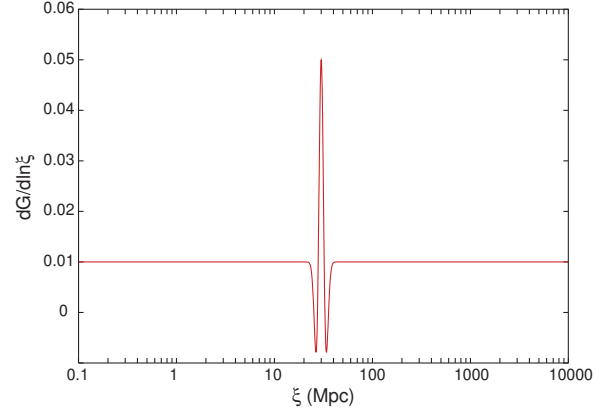


FIG. 8: The change of $dG/d\ln \xi$ as the function of ξ for a potential with a bump given by Eq. (27) for the case of $\lambda = 0.1, c = 10^{-6}, \nu = 100$ and $\xi_0 = 30$.

substituted into Eq. (8) to obtain a G as a function of ξ . This is shown in Fig. 8 for the parameters $\lambda = 0.1, c = 10^{-6}, \nu = 100$ and $\xi_0 = 30$.

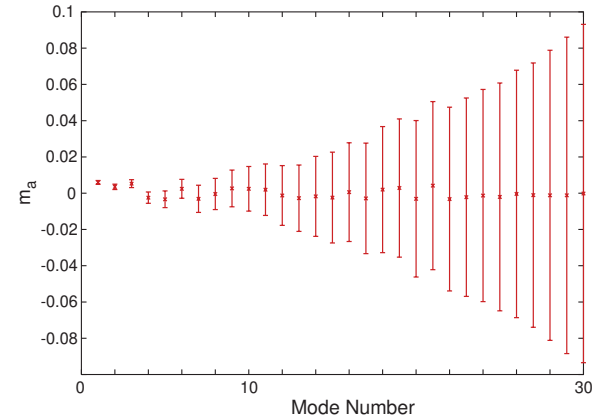


FIG. 9: The corresponding first 30 eigenmodes for the potential with a bump given by Eq. (27) for the case of $\lambda = 0.1, c = 10^{-6}, \nu = 100$ and $\xi_0 = 30$.

Convolving the $\{p_i\}$ shown in Fig. 8 with the eigenmodes in Fig. 4, we obtain the $\{m_a\}$ for this model; these are shown in Fig. 9. We see that only the first few modes have signal to noise bigger than unity. They therefore are all that need to be retained to capture the information necessary to distinguish this non-trivial potential from a perfectly flat potential. This is reasonable because, in this example, the deviation of $\frac{d}{d\ln \xi} G(\ln \xi)$ from zero occurs around the range of ξ to which only the well-constrained modes are sensitive.

V. CONCLUSION AND DISCUSSION

We applied a principal component analysis to the covariance matrix to investigate the precision with which CMB observables can ultimately constrain the inflaton potential, accounting for the uncertainties in cosmological parameters. We parametrized the inflaton potential using 200 parameters in the framework of the general slow-roll approximation without specifying any particular inflationary scenario. We showed that considering five principal components covering about four e-folds of conformal time will be sufficient to obtain almost all of the information on the features of the inflaton potential when the deviation from the flat potential is within $|dG/d\ln\xi| \lesssim 0.05$ in the scales CMB observables are sensitive to. We found the first principal component represents the local tilt and the second one the local running in the region around $k = 0.05 - 0.1 \text{ Mpc}^{-1}$ where cosmic variance limited CMB observations out to $l = 2000$ are most constraining.

We, however, should keep in our minds that the well constrained local “tilt” and “running” around $k \sim 0.1 \text{ Mpc}^{-1}$ does not determine the properties of $\mathcal{P}(k)$ or $V(\phi)$ more globally or assess the validity of either a constant tilt or constant running. This makes measuring $\mathcal{P}(k)$ at high k from non CMB sources more interesting.

ing since in the general context, the CMB says nothing about $n(k)$ beyond the compact support region of our best eigenmodes. Our formalism is general and can be easily extended to multiple data sets. For example, with small scale power spectrum information it may be interesting to marginalize a constant running as we did the tilt and construct the best eigenmode for the running of the running which can become rather important well beyond the few e-folds of the CMB range in the near future.

The principal component analysis helps clarify the particular aspects of the inflation potential that are well constrained. It is also a useful technique to find the optimal way of extracting information on the inflaton potential in a model independent manner in the analysis of actual data, say, via the Markov Chain Monte Carlo method once the polarization and higher angular resolution data becomes available in the future.

This work was supported by DOE, by NASA grant NAG5-10842, by the Packard Foundation, and by ARCSEC funded by Korea Science and Engineering Foundation and the Korean Ministry of Science, the Korea Research Foundation grant KRF PBRG 2002-070-C00022 and Brain Korea 21.

[1] C.L. Bennett et al., *Astrophys. J. Suppl.* **148** (2003) 1 [astro-ph/0302207]; D.N. Spergel et al., *Astrophys. J. Suppl.* **148** (2003) 148 [astro-ph/0302209]; H. Peiris et al., *Astrophys. J. Suppl.* **148** (2003) 213 [astro-ph/0302225]

[2] K. Abazajian et al., *Astron.J.* **126** (2003) 2081 [astro-ph/0305492]; ibid, *Astron.J.* **128** (2004) 502 [astro-ph/0403325]; D.G. York et al., *Astron.J.* **120** (2000) 1579 [astro-ph/0006396]

[3] M. Tegmark et al., *Phys.Rev.* **D69** (2004) 103501 [astro-ph/0310723]

[4] U. Seljak et al., [astro-ph/0407372]

[5] W. Hu and T. Okamoto, *Phys.Rev.* **D69** (2004) 043004 [astro-ph/0308049]

[6] P. Mukherjee and Y. Wang, *Astrophys.J.* **599** (2003) 1 [astro-ph/0303211]

[7] S.L. Bridle, A.M. Lewis, J. Weller and G. Efstathiou, *Mon. Not. Roy. Astron. Soc.* **342** (2003) L72 [astro-ph/030230]

[8] S. Hannestad, *JCAP* **0404** (2004) 002 [astro-ph/0311491]

[9] N. Kogo, M. Sasaki and J. Yokoyama, *Phys.Rev.* **D70** (2004) 103001 [astro-ph/0409052]

[10] M. Matsumiya, M. Sasaki and J. Yokoyama, *Phys.Rev.* **D65** (2002) 083007 [astro-ph/0111549]

[11] S. Habib, A. Heinen, K. Heitmann, G. Jungman and C. Molina-Paris, *Phys.Rev.* **D70** (2004) 083507 [astro-ph/0406134]; S. Habib, A. Heinen, K. Heitmann and G. Jungman, *Phys.Rev.* **D71** (2005) 043518 [astro-ph/0501130]

[12] E. Copeland, E. Kolb, A. Liddle and J. Lidsey, *Phys.Rev.* **D48** (1993) 2529 [hep-ph/9303288]; E. Copeland, E. Kolb, A. Liddle and J. Lidsey, *Phys.Rev.* **D49** (1994) 1840 [astro-ph/9308044]; J. Lidsey, A. Liddle, E. Kolb, E. Copeland, T. Barreiro and M. Abney, *Rev.Mod.Phys.* **69** (1997) 373 [astro-ph/9508078]; E. Copeland, I. Grivell, E. Kolb and A. Liddle, *Phys.Rev.* **D58** (1998) 043002 [astro-ph/9802209], A. Liddle and M. Turner, *D50* (1994) 758, Erratum-ibid *D54* (1996) 2980 [astro-ph/9402021]; For the experimental difficulties of detecting possible gravitational waves, see for example: L. Knox and Y. Song, *Phys.Rev.Lett.* **89** (2002) 011303 [astro-ph/0202286]; G. Efstathiou et al., [astro-ph/0503360]; D. Lyth, *Phys.Rev.Lett.* **78** (1997) 1861 [hep-ph/9606387]

[13] S. Habib, K. Heitmann and G. Jungman, *Phys.Rev.Lett.* **94** (2005) 061303 [astro-ph/0409599]

[14] M. Joy and E. Stewart, J. Gong and H. Lee, *JCAP* **04** (2005) 012 [astro-ph/0501659]

[15] I. Grivell, A. Liddle, *Phys.Rev.* **D61** (2000) 081301

[astro-ph/9906327]

[16] R. Easther and W. Kinney, **D67** (2003) 043511 [astro-ph/0210345]

[17] S. Dodelson and E. Stewart, Phys.Rev. **D65** (2002) 10130 [astro-ph/0109354]; E. Stewart, Phys.Rev. **D65** (2002) 103508 [astro-ph/0110322]; J. Choe, J. Gong and E. Stewart, JCAP **0407** (2004) 12 [hep-ph/0405155]

[18] L. Wang, V. Mukhanov and P. Steinhardt, Phys.Lett. **B414** (1997) 18 [astro-ph/9709032]

[19] A. R. Liddle and D. H. Lyth, *Cosmological inflation and large-scale structure* (Cambridge University Press, 2000).

[20] S. Dodelson, *Modern Cosmology* (Academic Press, San Diego, 2003).

[21] M. Tegmark, A. Taylor and A. Heavens, Astrophys.J. **480** (1997) 22 [astro-ph/9603021] ; M. Zaldarriaga, D. Spergel and U. Seljak, Astrophys.J. **488** (1997) 1 [astro-ph/9702157]